REJUVENATION RESEARCH
Volume 18, Number 1, 2015

DOI: 10.1089/rej.2014.1630

Restriction on an Energy-Dense Diet Improves Markers of Metabolic Health and Cellular Aging in Mice Through Decreasing Hepatic mTOR Activity

Anke Schloesser,[1] Graeme Campbell,[2] Claus-Christian Glüer,[2] Gerald Rimbach,[1] and Patricia Huebbe[1]

Abstract

Dietary restriction (DR) on a normal low-fat diet improves metabolic health and may prolong life span. However, it is still uncertain whether restriction of an energy-dense, high-fat diet would also be beneficial and mitigate age-related processes. In the present study, we determined biomarkers of metabolic health, energy metabolism, and cellular aging in obesity-prone mice subjected to 30% DR on a high-fat diet for 6 months. Dietary-restricted mice had significantly lower body weights, less adipose tissue, lower energy expenditure, and altered substrate oxidation compared to their *ad libitum*–fed counterparts. Hepatic major urinary proteins (Mup) expression, which is linked to glucose and energy metabolism, and biomarkers of metabolic health, including insulin, glucose, cholesterol, and leptin/adiponectin ratio, were likewise reduced in high-fat, dietary-restricted mice. Hallmarks of cellular senescence such as Lamp2a and Hsc70 that mediate chaperone-mediated autophagy were induced and mechanistic target of rapamycin (mTOR) signaling mitigated upon high-fat DR. In contrast to DR applied in low-fat diets, anti-oxidant gene expression, proteasome activity, as well as 5′-adenosine monophosphate–activated protein kinase (AMPK) activation were not changed, suggesting that high-fat DR may attenuate some processes associated with cellular aging without the induction of cellular stress response or energy deprivation.

Introduction

Dietary restriction (DR), a reduction of food or calorie consumption along with sufficient micronutrient intake, has been applied as useful intervention strategy to reduce body weight and prevent obesity-related pathologies.[1,2] Moreover, DR effectively decelerates aging and increases life span in model organisms, including yeast, nematodes, flies, and laboratory rodents. Metabolic reprogramming through reducing activity of nutrient-sensing pathways such as target of rapamycin (TOR), insulin/insulin-like growth factor 1 (IGF-1), and Ras–adenylate cyclase (AC)–protein kinase A (PKA) signaling, as well as increase of sirtuin 1 (SIRT1) activity has been proposed to, at least partly, underlie the life-extending ability of DR.[3,4] Downstream of these molecules are proteins involved in anti-oxidant, xenobiotic, and endoplasmic reticulum stress response, autophagy, or glucose and fatty acid metabolism. However, there is growing evidence that not only reduced calorie intake alone but also macronutrient balance of the diet may actually define DR-related response. It seems that low protein (5%–15%) and high carbohydrate intakes (40%–60%) could promote health and life span in fruit flies, mice, and humans.[5–7] Recent data indicate that lipid composition can also impact the life span of mice subjected to DR.[8]

In dietary-restricted rodents, monkeys, and humans, blood pressure and plasma levels of insulin, leptin, C-reactive protein (CRP), triglycerides, and cholesterol are reduced, thereby improving insulin sensitivity and cardiometabolic health.[9–15] The first results of long-term DR in long-lived primates show promising effects on health status and age-related disease pathologies and mortality,[16–19] whereas a contrasting study found no beneficial effects on all-cause or age-related mortality, although an improvement in health span.[13] It is of note that clear longevity-related effects in the DR group are particularly absent when the control group is fed a limited amount of food to prevent hyperphagia,[13] and the question was raised whether beneficial effects of DR, at least in primates, may only be due to the elimination of excess fat intake.[20] Interestingly, the positive health-promoting effects observed in the few human studies were observed when dietary-restricted

[1]Institute of Human Nutrition and Food Science and [2]Section Biomedical Imaging, Department of Diagnostic Radiology, University of Kiel, Kiel, Germany.

subjects were compared to controls that were on typical Western diets containing 30%–40% energy from fat, whereas DR was achieved by consumption of nutrient-dense foods with low fat contents (11%–28% energy from fat).[14,15,21] Protein and carbohydrate percentages of the DR diets were strikingly inconsistent and varied between 12% and 28% for energy from protein and 46%–77% for energy from carbohydrates, although similar changes in blood lipids, blood pressure, or insulin were observed.[14,15,22] Therefore, we raised the question whether DR on a Western-type diet with high fat (42%) but also relatively high carbohydrate (43%) and low protein content (15%) may still exert positive effects on metabolic health and longevity-related signaling pathways in mice.

In the present study, we determined biomarkers of metabolic health, energy metabolism, and cellular senescence in mice subjected to 6 months of DR on a high-fat and high-sugar Western-type diet. Moreover, we aimed at evaluating modulation of nutrient-sensing signaling pathways by high-fat DR (HFDR) in comparison with known effects observed in DR mice on regular low-fat diets (LFD).

Materials and Methods

Mice and diet

Animal studies were performed according to German regulations of animal welfare and with permission of the appropriate local authorities.

Male C57BL/6J mice, 6–8 weeks old, were purchased from Taconic Europe A/S (Ry, Denmark). The mice were housed individually in Macrolon cages under controlled environmental conditions (22–24°C, 45%–55% relative humidity, 12-hr light/dark cycle) and had free access to diet and water. The experimental diet was a purified semi-synthetic, energy-dense, high-fat, and high-sugar diet purchased from Ssniff (TD 88137 modified; Soest, Germany) that is known to rapidly induce body weight gain and adipose tissue hypertrophy in C57BL/6 mice.[23] The diet contained 17.1 grams/kg crude protein, 21.2 grams/kg crude fat, 14.5 grams/kg starch, and 32.8 grams/kg sucrose. The metabolizable energy of the diet (19.1 MJ/kg) was composed of 43% carbohydrates, 15% protein, and 42% fat with a protein-to-carbohydrate ratio of 0.35. After 1 week of *ad libitum* feeding, the mice were divided by body weight into two weight-matched groups ($n = 6$), one *ad libitum*–fed (AL) and one DR group. The DR group was fed 70% of the food amount consumed by the AL group calculated on a weekly basis for 6 months. DR was gradually introduced in a preceding adaptation phase, meaning a reduction of food intake by 5% each week until the final restriction of 30% was reached. Food intake and body weight were determined on a daily and weekly basis, respectively. After 6 months of 30% DR, the mice (10 months of age) were killed by cervical dislocation, and blood was immediately collected from the heart using a heparin-coated syringe and placed on ice for 30 min. Plasma was obtained by centrifugation ($3000 \times g$, 10 min, 4°C) and stored at −80°C until analysis. Liver was removed, snap frozen in liquid nitrogen, and stored at −80°C until analysis (except for samples for RNA isolation which were put in RNAlater [Qiagen, Hilden, Germany] and stored at −20°C).

Energy expenditure and respiratory exchange ratios by indirect calorimetry

Energy expenditure (EE) and respiratory exchange ratios (RER) of three mice per group were assessed in triplicate measurements after 2 and 4 months of the dietary intervention. Volumes of O_2 consumption (VO_2) and CO_2 production (VCO_2) were measured using the TSE PhenoMaster (TSE Systems GmbH, Bad Homburg, Germany). Mice were placed in respiratory chambers for 48 hr (including 24 hr of adaptation) with an airflow of 0.35 L/min and air sampling every 15 min for O_2 and CO_2 analysis. EE and RER were calculated as follows: $EE = (3.941 * VO_2 + 1.106 * VCO_2) * 4.1868/1000$ and expressed as $kJ/(h * kg^{0.75})$; $RER = VCO_2/VO_2$.

Body composition by micro-computed tomography

Micro-computed tomography (micro-CT) was used to determine the volume of visceral and subcutaneous adipose tissue of high-fat mice at the age of 6 months. Three mice per group were anesthetized with ketamine/xylazine, and the abdominal region between the first and the fifth lumbar vertebra was scanned using a conebeam *in vivo* micro-CT system (vivaCT 40 Scanner, Scanco Inc., Bruettisellen, Switzerland). The scan was performed using the following parameters: Energy settings of the X-ray source 45 kVp and 177 μA, voxel size 76 μm, integration time 300 msec, 250 projections per 180°. Subcutaneous and visceral adipose tissue volumes were calculated with an algorithm adapted from Lublinsky et al. (2009),[24] which uses canny edge detection and mathematical morphological operations (http://bme.sunysb.edu/labs/sjudex/miscellaneous.html). Adaptations included an additional dilation sequence of 3 voxels prior to component labeling to remove the background of the body image and the increase of the close distance in generating the mask for the visceral fat from 26 to 30. The volumes of the final masks generated from the algorithm were determined with the standard analysis program provided by Scanco.

Plasma biomarkers and hepatic lipid content

Fasted plasma concentrations of leptin (R&D Systems, Abingdon, UK), adiponectin (Abcam, Cambridge, UK), and insulin (Merck Millipore, Darmstadt, Germany) were measured using commercially available enzyme-linked immunosorbent assay (ELISA) kits. The fasted plasma concentration of glucose was determined with a colorimetric assay (Cayman, Ann Arbor, MI) using enzymatic oxidation of glucose to δ-gluconolactone by flavin adenine dinucleotide (FAD)-dependent reduction of glucose oxidase and subsequent production of hydrogen peroxide. Plasma and liver triglyceride and cholesterol concentrations were analyzed enzymatically using Fluitest®TG and Fluitest®Chol kits (Analyticon, Lichtenfels, Germany). Liver lysates were prepared as described previously[25,26] using 50 mg of frozen liver and elution with hexane/isopropanol (see Supplementary Data, available at www.liebertonline.com/rej/). Plasma was used directly without any pretreatment.

Hepatic gene expression using quantitative reverse transcriptase PCR

For RNA isolation and purification, a miRNA NucleoSpin® Kit (Macherey & Nagel, Düren, Germany) for parallel

isolation of small (<200 bases) and large (>200 bases) RNA was used. The concentration of isolated RNA was determined by measuring the absorbance at 260 nm, and the purity was determined by the ratios of 260/280 nm (~2.0) and 260/230 nm (2.0–2.2) with a NanoDrop spectrophotometer (Thermo Scientific, Peqlab Biotechnologie GmbH). RNA was diluted to a final concentration of 100 ng/μL and stored in aliquots at −80°C until quantitative reverse transcriptase PCR (qRT-PCR) analysis. Primers for qRT-PCR were designed using Primer3 Input software (v. 0.4.0) and purchased from Eurofins MWG (Ebersberg, Gemany) (Table S1). One-step qRT-PCR was carried out with the SensiMix™ SYBR No-ROX One-Step Kit (Bioline, Luckenwalde, Germany) and with SYBRGreen detection on a Rotorgene 6000 cycler (Corbett Life Science, Sydney, Australia). Relative mRNA levels were calculated with an external standard curve and related to the mean of housekeeping gene expression (mean of *Rn18S* and *Eef2).*

Hepatic protein expression using western blotting

Protein expression was determined in cytosolic lysates prepared from fresh liver tissue except for phospho-Akt and Akt levels, which were detected in whole-cell lysates (see Supplementary Data). A total of 60 μg and 70 μg, respectively, protein of each sample was mixed with loading buffer (Table S2), denatured at 95°C for 5 min and loaded on Criterion™ TGX Stain-Free™ Precast Gels (BioRad, Munich, Germany) for separation by sodium dodecyl sulfate polyacrylamide gel electrophoresis (SDS-PAGE). Protein fluorescence was activated by ultra-violet (UV) exposition for 5 min before transfer onto a polyvinylidene fluoride (PVDF) membrane using the Trans Blot® Turbo™ System (BioRad, Munich, Germany). Target proteins were identified using respective primary (Table S3) and secondary antibodies (Santa Cruz Biotechnoloy, Heidelberg, Germany), visualized with enhanced chemiluminescence (ECL) reagents (Fisher Scientific, Schwerte, Germany) in a ChemiDoc XRS system (BioRad, Munich, Germany). Band intensities were calculated with Image Lab 4.1 software (BioRad). Target protein expression was related to the total protein load per lane, which was assessed by UV-induced (UV light exposure of the gel in a ChemiDoc XRS system for 5 min) reaction of trihalo compounds with tryptophan residues measured as PVDF membrane fluorescence after transfer of protein. Prior to data analysis, critical protein load was determined to avoid saturated fluorescence signals by establishing a dose-dependent relationship between protein load and fluorescence signal.[27]

Hepatic proteasome activity

A total of 20 mg of frozen liver tissue was homogenized in 180 μL of ice-cold lysis buffer (pH 7.8) for 2×2 min at 25 Hz with the TissueLyser II and incubated on ice for 30 min. Subsequently, the homogenates were centrifuged (15,700×*g* for 10 min at 4°C), and the supernatant was used. Fifty micrograms of protein (5 μL) of each sample was incubated with 190 μL of reaction buffer (pH 7.8) and 5 μL of the fluorescent substrate *N*-succinyl-leucine-leucine-valine-tyrosine-7-amino-4-methylcoumarin (Suc-LLVY-AMC, Enzo Life Sciences, Loerrach, Germany). The initially quenched fluorescence signal was released following cleavage of the substrate by the specific proteasome active site and was measured on a Tecan Infinite F200 plate reader (Tecan, Grödig, Austria) at 360 nm and 465 nm excitation and emission wavelengths. Calculation of proteasome activity was based on an external standard curve generated with the free fluorescent probe AMC (Enzo Life Sciences).

Statistical analysis

All presented data were calculated as means ± standard error of the mean (SEM). Data were analyzed for normality of distribution (Kolmogorov–Smirnov and Shapiro–Wilk tests) and equality of variances (Levene test) prior to the Student *t*-test. In the absence of normal distributed data, the Mann—Whitney U-test was applied. Values of $p < 0.05$ were considered statistically significant and indicated as asterisks (*). The statistical analysis was performed using PASW Statistics 18 (IBM, Chicago, IL).

Results

HFDR reduces body weight, adipose tissue volume, energy expenditure, and hepatic major urinary protein levels and improves metabolic health parameters in plasma

AL group mice significantly gained body weight during the study period (26.5 ± 0.7 vs. 37.8 ± 2.1 grams; $p = 0.001$), whereas the body weight of DR mice was significantly lower compared to the initial body weight (25.9 ± 0.6 vs. 23.5 ± 0.6 grams; $p = 0.005$; Fig. 1A). From week 4 of the intervention period, the difference in body weight between the groups was statistically significant ($p \leq 0.004$). EE and RER were assessed after 2 and 4 months of dietary intervention. The EE of DR mice was lower in the dark phase compared to AL mice after 2 and 4 months of intervention (Fig. 1B), suggesting a deliberate reduction of locomotor activity in the active phase due to shortage of dietary energy intake. The decrease in the RER that is statistically significant after 4, but not 2, months indicates a shift from mixed substrate to fat oxidation (Fig. 1C) and an increased mobilization of stored triglycerides from adipose tissue (AT) in the DR mice, which is visible in the apparently reduced volumes of visceral (118 vs. 2048 mm^3) and subcutaneous (358 vs. 1131 mm^3) AT as compared to AL mice (Fig. 1D, E). Energy deprivation under HFDR led to a significant suppression of hepatic major urinary proteins (Mup) expression (Fig. 1F). Furthermore, plasma levels of glucose, insulin, cholesterol, leptin, and the leptin-to-adiponectin ratio were reduced, indicating an improvement of metabolic health parameters (Table 1).

HFDR increases hepatic gluconeogenic but decreases lipogenic gene expression

In response to the restricted calorie intake, hepatic energy metabolism of HFDR mice was shifted toward gluconeogenesis with significant transcriptional induction of the key enzymes phosphoenolpyruvate carboxykinase 1 ($p = 0.035$) and glucose 6-phosphatase ($p = 0.003$). At the same time, expression of genes encoding enzymes involved in fatty acid synthesis, such as *Fasn* ($p = 0.008$), *Scd1* ($p < 0.001$), and *Fads1* ($p = 0.004$), was significantly reduced decelerating hepatic lipid synthesis (Table 2).

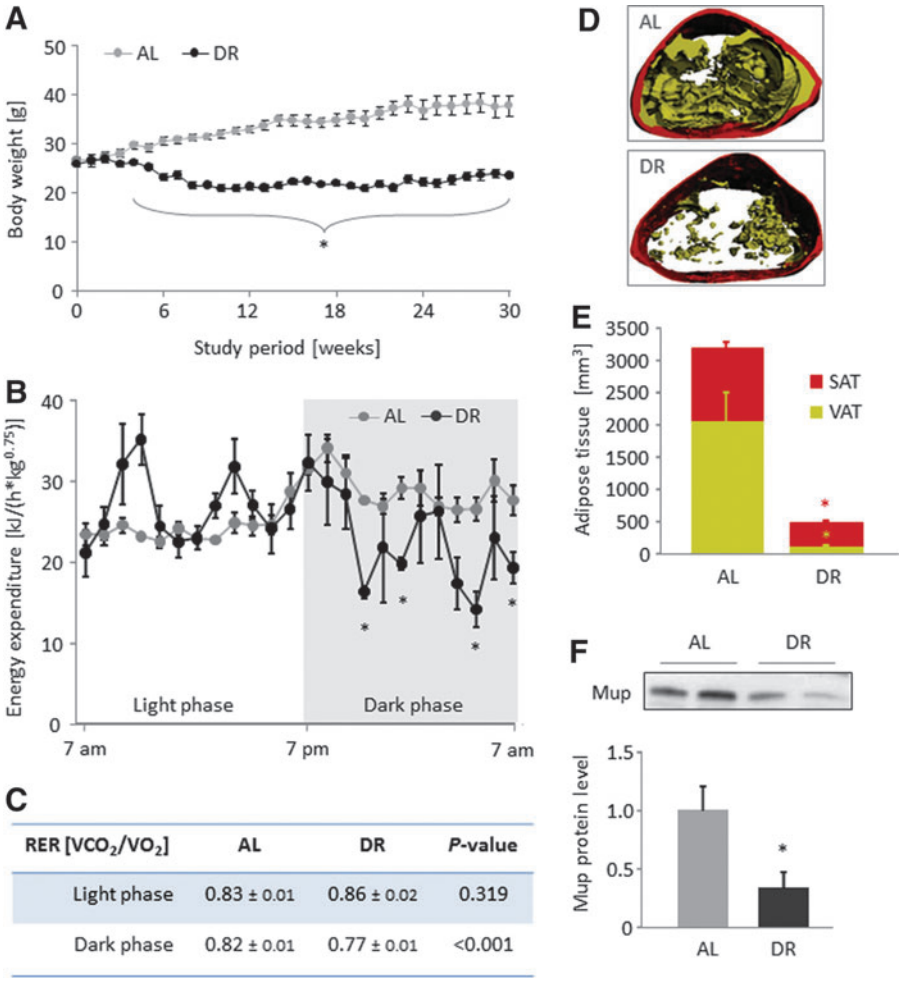

FIG. 1. High-fat dietary restriction (HFDR) reduces body weight, adipose tissue volume, energy expenditure, and hepatic major urinary proteins (Mup) levels. Body weight development of HFDR and *ad libitum*–fed (AL) mice (**A**). Energy expenditure (**B**) and respiratory exchange ratio (RER) (**C**) assessed by indirect calorimetry of DR compared to AL mice after 4 months of intervention. Adipose tissue volume was assessed using micro-computed tomography (micro-CT) after 4 months of intervention. Two images representative for the differences in adipose tissue volume fraction observed are shown (**D**). Subcutaneous fat is illustrated as dark and visceral fat as light gray area. Group means of subcutaneous adipose tissue (SAT) and visceral adipose tissue (VAT) volumes are shown (**E**). Hepatic Mup protein levels in DR and AL mice were determined by western blotting, and a representative blot is shown (**F**). Mup protein bands were analyzed densitometrically, and values were related to the total protein fluorescence signal on the blotting membrane. All values are means ± standard error of the mean (SEM) (six animals per group for body weight and Mup protein level, three animals per group for micro-CT, EE, and RER analyses). (*) Significant difference ($p < 0.05$ by *t*-test) between AL and DR mice. VCO_2, volume of CO_2 production; VO_2, volume of O_2 consumption. Color images available online at www.liebertpub.com/rej

Table 1. Metabolic Plasma Parameters after 6 Months of High-Fat Dietary Restriction

	AL	*DR*	p *value*
Glucose (mg/dL)	214 ± 13	131 ± 9	*< 0.001*
Insulin (mU/L)	42.6 ± 6.5	14.1 ± 0.7	*0.004*
Triglycerides (mg/dL)	42.7 ± 13.7	57.7 ± 8.9	*0.367*
Cholesterol (mg/dL)	234 ± 33.9	105 ± 6.9	*0.008*
Adiponectin (μg/mL)	10.0 ± 1.0	14.2 ± 0.9	*0.010*
Leptin (ng/mL)	34.8 ± 7.4	1.1 ± 0.3	*0.006*
Leptin/adiponectin	3.44 ± 0.81	0.08 ± 0.02	*0.009*

Values are means ± standard error of the mean (SEM) from six mice per group.

AL, *ad libitum*–fed; DR, dietary restriction.

HFDR induces heat shock genes and chaperone-mediated autophagy, but does not affect proteasome activity or anti-oxidant gene expression

Aging is associated with altered expression of heat shock protein gene family members such as Hsp70 and Hsc70,[28,29] whereas HFDR significantly induced their mRNA level (Table 2). In addition, Lamp2a protein expression was two-fold higher in restricted than AL-fed mice ($p = 0.022$; Fig. 2A), indicating a stimulation of chaperone-mediated autophagy upon HFDR. In contrast, protein levels of the macro-autophagy markers LC3 I and II as well as proteasome activity were not different between HFDR and AL mice (Fig. 2B, D). Relative mRNA levels of the protein folding and endoplasmic reticulum (ER) stress markers

Table 2. Relative Hepatic mRNA Levels in High-Fat Dietary Restricted Compared to *Ad Libitum*–Fed Mice

	Gene	*AL*	*DR*	p *value*
Gluconeogenesis				
Phosphoenolpyruvate carboxykinase 1	*Pck1*	0.67 ± 0.07	1.05 ± 0.14	*0.035*
Glucose-6-phosphatase	*G6pc*	1.31 ± 0.20	3.32 ± 0.48	*0.003*
Lipogenesis				
Fatty acid synthase	*Fasn*	1.37 ± 0.11	0.79 ± 0.14	*0.008*
Stearoyl-coenzyme A desaturase 1	*Scd1*	1.57 ± 0.18	0.43 ± 0.08	*< 0.001*
Fatty acid desaturase 1	*Fads1*	1.51 ± 0.17	0.71 ± 0.08	*0.004*
Heat shock proteins				
Hsp70	*Hspa1b*	1.42 ± 0.11	10.50 ± 2.81	*0.009*
Hsc70	*Hspa8*	1.17 ± 0.13	2.01 ± 0.15	*0.002*
Unfolded protein response				
Bip/Grp78	*Hspa5*	1.41 ± 0.17	0.98 ± 0.13	*0.074*
Protein disulfide isomerase	*Pdia3*	1.08 ± 0.09	0.41 ± 0.06	*< 0.001*
Anti-oxidant defense				
Catalase	*Cat*	0.83 ± 0.10	0.67 ± 0.06	*0.196*
Superoxide dismutase 1	*Sod1*	1.13 ± 0.06	1.23 ± 0.07	*0.318*
Glutathione peroxidase 1	*Gpx1*	0.93 ± 0.16	1.21 ± 0.11	*0.175*
Glutathione peroxidase 4	*Gpx4*	1.24 ± 0.14	1.26 ± 0.14	*0.899*
NAD(P)H-quinone oxidoreductase 1	*Nqo1*	1.06 ± 0.18	0.85 ± 0.11	*0.337*
Gamma-glutamylcysteine synthetase, heavy chain (catalytic subunit)	*Gclc*	1.39 ± 0.05	1.30 ± 0.16	*0.651*
Gamma-glutamylcysteine synthetase, light chain (modifier subunit)	*Gclm*	1.15 ± 0.14	1.39 ± 0.23	*0.386*

Values are means ± standard error of the mean (SEM) from six mice per group.
AL, *ad libitum*–fed; DR, dietary restriction.

Pdia3 and Bip/Grp78 were significantly ($p < 0.001$) or rather in trend lower ($p = 0.074$) in HFDR mice (Table 2), whereas Bip/Grp78 protein levels were similar in all mice (Fig. 2C). Finally, mRNA levels of genes encoding for anti-oxidant enzymes were not modulated by HFDR in our mice (Table 2).

mTOR activation and insulin-related signaling are diminished upon HFDR

The signaling pathway of the mechanistic target of rapamycin (mTOR) involves activation of several up- and down-stream targets, including the serine/threonine protein kinases S6K1 and Akt. Phosphorylated (activated) protein levels of mTOR, S6K1, and Akt were significantly lower in HFDR mice, with similar total protein levels (Fig. 3A–C) suggesting diminished activity of the mTOR pathway. Protein levels of phosphorylated and total AMPK, which recognizes the intracellular andenosine triphosphate/adenosine monophosphate (ATP/AMP) ratio, were not different between restricted and AL-fed mice (Fig. 3D). These data emphasize a normalization of mTOR signaling compared to unrestricted HFD feeding without occurrence of intracellular energy deprivation.

Discussion

In the present study, we applied DR using an energy-dense diet rich in fat and sugar (Western-type diet) with a low protein-to-carbohydrate ratio to reduce body weight and fat mass in obesity-prone C57BL/6 mice. The HFDR ameliorated metabolic dysfunction and mitigated hyper-activation of growth factor–related signaling, such as mTOR and insulin. Our data indicate that a simple reduction of the absolute intake of an otherwise adverse diet[23] may improve metabolic health and impede cellular aging, *e.g.* through induction of chaperone-mediated autophagy. In contrast to DR regimens applied on standard rodent chows with low-fat content and high protein-to-carbohydrate ratios,[11] the HFDR is, however, not provoking metabolic stress signals that would include activation of AMPK, anti-oxidant, or ER stress response.

In this study, DR resulted in a significant decrease of the adjusted total EE in the dark phase, which implies that DR mice reduced their physical activity during their active phase. These data point to an adaptation to the reduced energy intake by limiting physical activity and not only to a reduction of EE due to the loss of body weight or energy consuming lean mass. Nevertheless, literature data about the impact of DR on EE and physical activity in rodents are not consistent and may comprise either reduced activity likely to save energy or hyper-activity, presumably due to increased food seeking.[30] The RER, which is a measure of the fuel substrate used in mitochondrial oxidation, was likewise decreased in the dark phase, averaging 0.7. This is indicative of increased fatty acid oxidation, supporting the assumption that DR mice reduced their physical activity in response to food shortage compared to AL mice.

Previous reports have already suggested that 6–10 weeks of DR on a high-fat diet can improve metabolic health parameters including reduction of plasma insulin, glucose, and leptin levels similar to low-fat diets,[31–33] although HFDR for shorter periods (3 weeks) may be rather marginally effective.[34] In contrast to other HFDR studies that focused on white adipose tissue[33,35] and arterial function,[9] we investigated potential longevity-related and nutrient-sensing pathways in the liver on 6 months of HFDR. In our study, activity of the key nutrient-sensing mTOR pathway was significantly reduced through HFDR, including less

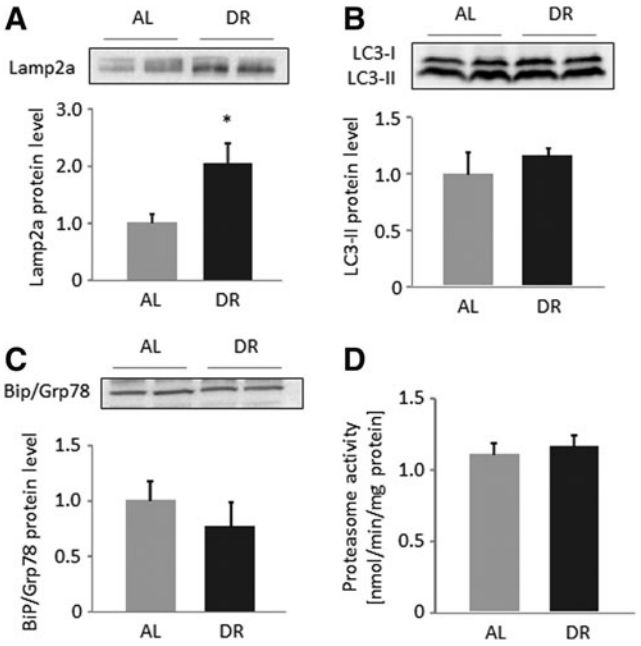

FIG. 2. High-fat dietary restriction (HFDR) induces Lamp2a, a lysosomal protein involved in chaperone-mediated autophagy (CMA). Hepatic protein levels of the CMA Lamp2a (**A**) and the macro-autophagy markers LC3-I and II (**B**) as well as the unfolded protein response marker BiP/Grp78 (**C**) were determined by western blotting, and densitometric analysis of target bands of DR was compared to *ad libitum*–fed (AL) mice. Target protein expression was related to the total protein fluorescence assessed on the blotting membrane. Representative blots from two out of six animals per groups are shown. Densitometric values are means + standard error of the mean (SEM) from six animals per group. Proteasome activity was measured in liver lysates of all animals and group means + SEM are shown (**D**). (*) Significant difference ($p < 0.05$ by *t*-test) between AL and DR mice.

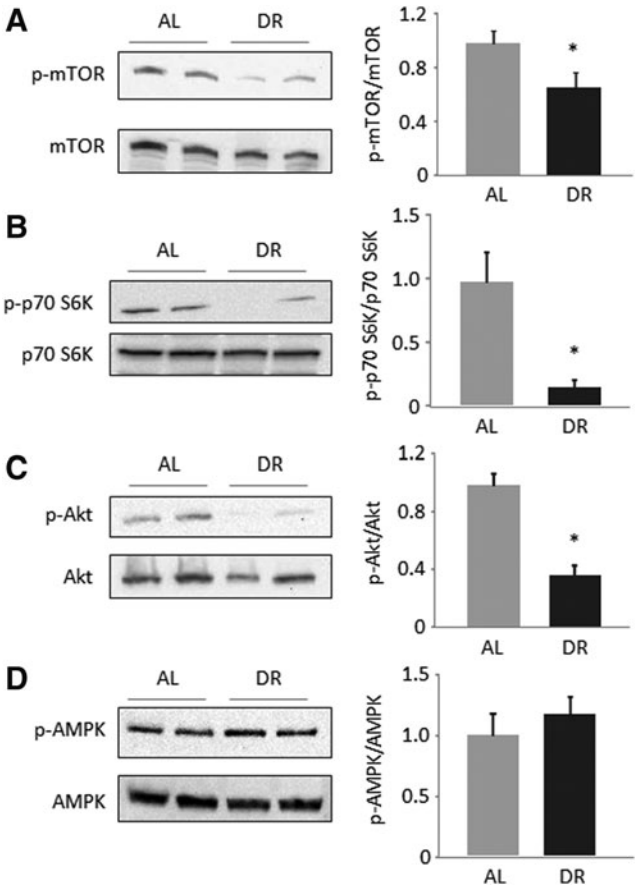

FIG. 3. Mechanistic target of rapamycin (mTOR) activation and insulin-related signaling are diminished upon high-fat dietary restriction (HFDR). Hepatic protein levels of phosphorylated and total mTOR (**A**), phosphorylated and total p70 S6 kinase (S6K) (**B**), phosphorylated and total Akt (**C**), and phosphorylated and total AMP-activated protein kinase (AMPK) (**D**) were determined by western blotting and subsequent densitometric analysis of target bands. Target protein expression was related to the total protein fluorescence transferred to the polyvinylidene fluoride (PVDF) membrane, and the ratio of phosphorylated forms to total target protein was calculated as measure of target protein activation. Representative blots from two out of six animals per groups are shown. Densitometric values are means + standard error of the mean (SEM) from six animals per group. (*) Significant difference ($p < 0.05$ by *t*-test) between *ad libitum*–fed (AL) and dietary-restricted (DR) mice.

activation of its downstream targets S6 kinase and Akt. The mTOR pathway is activated by nutrients (*e.g.* branched amino acids), insulin, and growth factors and inhibited by dropping cellular energy levels and other stress signals involving AMP-activated protein kinase (AMPK).[35] Constant abundance of nutrients and dietary energy, as during high-fat diet consumption, leads to excessive mTOR activation; therefore, in our HFDR mice, the reduction and normalization of mTOR signaling was most likely due to the reduced intake of dietary energy and protein but also reduced insulin secretion. Cellular aging is a function of mTOR activity,[36,37] implying that aging processes are decelerated under HFDR compared to *ad libitum* consumption (Fig. 4).

In the present study, different hallmarks of cellular aging were normalized in HFDR compared to AL mice, including expression of heat shock proteins (Hsp70, Hsc70) and Lamp2a. Hsc70 and Lamp2a mediate the so-called chaperone-mediated autophagy (CMA), which is a selective autophagic pathway for one-by-one sequestration of individual proteins and subsequent degradation in lysosomes. Similar to micro- and macro-autophagy, the main function of CMA is the removal of unfolded damaged proteins, and its activity is known to decrease by age.[38,39] Low-fat DR induces Hsc70 transcription in livers of old rats,[40] and age-dependent decline in Lamp2a expression is attenuated by inhibition of mTOR.[41] Therefore, it is reasonable to suggest that the observed effects on CMA markers are due to reduced mTOR activity in our mice. Interestingly, there were no differences in LC3 expression observed between DR and AL mice, suggesting that macro-autophagy was not modulated by HFDR in our study. This is in contrast to other studies, where induction of LC3-related autophagy was found in muscle after HFDR [31] and in liver after low-fat DR.[11]

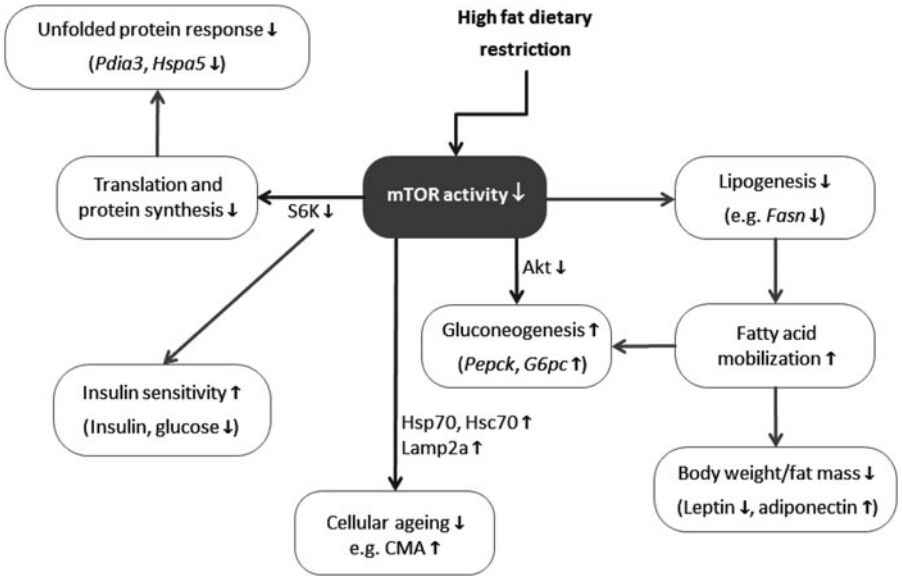

FIG. 4. Effects of high-fat dietary restriction (HFDR) are mediated through reduced mechanistic target of rapamycin (mTOR) activity. By reducing mTOR activity, anabolic processes such as protein translation, gluconeogenesis, and lipogenesis are decreased, which reduces protein synthesis and fat mass. Due to reduced protein assembly, protein folding capacity and unfolded protein response are diminished. Reduced mTOR activity is associated with normalization of aberrant insulin signaling and decelerated cellular aging, *e.g.*, a restoration of levels of chaperone-mediated autophagy (CMA) markers, such as Hsc70 and Lamp2a. Direct targets of HFDR through mTOR are depicted in blue; indirect targets are shown in yellow. Up- or down-regulation of targets and processes in response to HFDR as compared to *ad libitum*–fed controls is indicated by vertical arrows (down ↓, up ↑).

In contrast to Hsp70 and Hsc70, other heat shock proteins, namely ER chaperones, have been found to be transcriptionally down-regulated in the liver under calorie restriction conditions.[42–44] ER chaperones (*e.g.*, BiP/Grp78) together with other ER proteins (*e.g.*, Pdia3) mediate the proper folding of newly synthesized or damaged misfolded proteins, a process that is termed unfolded protein response (UPR). If the folding capacity is overloaded, misfolded proteins will be conveyed to proteasome or lysosomal (macro-autophagic) degradation. The UPR may be either a consequence of accumulation of damaged proteins provoked by stress (*e.g.*, pharmacological agents) or of accumulation of nascent proteins through increased synthesis under physiological conditions. In the latter case, mTOR activation[45,46] and growth factor signaling[47] are mainly responsible for induction of UPR in liver cells. In our HFDR mice, expression of the UPR members Bip/Grp78 and Pdia3 was lower compared to AL mice, whereas proteasome activity and LC3-related autophagy were not different. These data suggest that the newly synthesized protein folding load was reduced due to curbed mTOR activity and protein synthesis upon HFDR.

The reduced activation of one of the main downstream targets of mTOR, S6 kinase 1 (S6K1), is also associated with improved insulin signaling because S6K1 induces degradation of the insulin receptor substrate 1 and thereby leads to reduced insulin sensitivity.[48,49] Normalization of insulin signaling was observed as significantly reduced plasma insulin and glucose levels as well as a lower leptin/adiponectin ratio in our HFDR mice. Furthermore, insulin-dependent activation of the mTOR/Akt pathway triggers lipogenesis and inhibits gluconeogenesis in the liver[50,51]; therefore, attenuation of insulin/mTOR/Akt signaling may have led to the transcriptional inhibition of lipogenic and induction of gluconeogenic genes upon HFDR (Fig. 4).

In contrast to the genes of hepatic energy metabolism, genes involved in anti-oxidant defense were not differentially regulated in response to HFDR. As previously shown, DR applied on a LFD led to an induction of anti-oxidant genes, which was also observable on the protein and activity levels[11]; however, in the majority of published studies, DR had little or no effects on reactive oxygen species (ROS) production and anti-oxidant activity.[52] These data suggest that the anti-aging effect of DR is not essentially attributable to anti-oxidant effects and that aging is not a consequence of oxidative stress but rather casually accompanied by accumulating oxidative damages.[53] According to the theory of TOR-driven aging that implies the constant activation of the TOR signal transduction pathway in mature cells leading to cellular senescence,[36,53] HFDR may certainly represent a useful anti-aging strategy through inhibition of mTOR,[54] even in the absence of anti-oxidant defense induction. This is in line with recent findings in adult mice showing that DR reduces the number of senescent cells in tissues, including the liver, together with improved telomere maintenance but without actually increasing telomerase activity.[55]

It is assumed that DR-induced life-span extension is based on an interplay between nutrition and reproduction[12] and there is evidence linking steroid signaling to nutrient-sensing pathways involving TOR.[56] In the present study, hepatic Mup expression was significantly reduced in dietary-restricted mice comparable to restricted mice on a LFD.[12]

Mup are scent marks controlling sexual maturation of mice[57] that have also been implicated in nutritional processes such as glucose and energy metabolism.[58] Therefore, it is likely that nutrient-dependent Mup expression is also regulated through mTOR, suggesting that decelerating cellular senescence is associated with life span extension in mice and may be achieved through HFDR.

In conclusion, HFDR attenuates mTOR activity and normalizes nutrient-dependent signaling, thereby decelerating cellular senescence and improving the metabolic health status. Considering the fact that a healthy diet generates low mTOR activation and insulin levels,[5] it is reasonable that simply restricting the absolute amount ingested of a Western-type diet may already improve health and thereby delay the aging process.

Acknowledgments

This study was supported financially by a grant of the German Ministry of Education and Science (BMBF 0315681) entitled ''Aetiology, pathophysiology and prevention of catching up body fat mass after body weight reduction: Avoiding yo-yo effects in the treatment of obesity.''

Author Disclosure Statement

No competing financial interests exist.

References

1. Hocman G. Prevention of cancer: Restriction of nutritional energy intake (joules). Comp Biochem Physiol A Comp Physiol 1988;91:209–220.
2. Bales CW, Kraus WE. Caloric restriction: Implications for human cardiometabolic health. J Cardiopulm Rehabil Prev 2013;33:201–208.
3. Fontana L, Partridge L, Longo VD. Extending healthy lifespan—from yeast to humans. Science 2010;328:321–326.
4. Wang Y. Molecular links between caloric restriction and Sir2/SIRT1 activation. Diabetes Metab J 2014;38:321–329.
5. Solon-Biet SM, McMahon AC, Ballard JW, Ruohonen K, Wu LE, Cogger VC, Warren A, Huang X, Pichaud N, Melvin RG, Gokarn R, Khalil M, Turner N, Cooney GJ, Sinclair DA, Raubenheimer D, Le Couteur DG, Simpson SJ. The ratio of macronutrients, not caloric intake, dictates cardiometabolic health, aging, and longevity in ad libitum-fed mice. Cell Metab 2014;19:418–430.
6. Levine ME, Suarez JA, Brandhorst S, Balasubramanian P, Cheng CW, Madia F, Fontana L, Mirisola MG, Guevara-Aguirre J, Wan J, Passarino G, Kennedy BK, Wei M, Cohen P, Crimmins EM, Longo VD. Low protein intake is associated with a major reduction in IGF-1, cancer, and overall mortality in the 65 and younger but not older population. Cell Metab 2014;19:407–417.
7. Couzin-Frankel J. Nutrition. Diet studies challenge thinking on proteins versus carbs. Science 2014;343:1068.
8. Lopez-Dominguez JA, Ramsey JJ, Tran D, Imai DM, Koehne A, Laing ST, Griffey SM, Kim K, Taylor SL, Hagopian K, Villalba JM, Lopez-Lluch G, Navas P, McDonald RB. The influence of dietary fat source on lifespan in calorie restricted mice. J Gerontol A Biol Sci Med Sci 2014;glu177.
9. Donato AJ, Walker AE, Magerko KA, Bramwell RC, Black AD, Henson GD, Lawson BR, Lesniewski LA, Seals DR. Life-long caloric restriction reduces oxidative stress and preserves nitric oxide bioavailability and function in arteries of old mice. Aging Cell 2013;12:772–783.
10. Okauchi N, Mizuno A, Yoshimoto S, Zhu M, Sano T, Shima K. Is caloric restriction effective in preventing diabetes mellitus in the Otsuka Long Evans Tokushima fatty rat, a model of spontaneous non-insulin-dependent diabetes mellitus? Diabetes Res Clin Pract 1995;27:97–106.
11. Giller K, Huebbe P, Hennig S, Dose J, Pallauf K, Doering F, Rimbach G. Beneficial effects of a 6-month dietary restriction are time-dependently abolished within 2 weeks or 6 months of refeeding-genome-wide transcriptome analysis in mouse liver. Free Radic Biol Med 2013;61C:170–178.
12. Giller K, Huebbe P, Doering F, Pallauf K, Rimbach G. Major urinary protein 5, a scent communication protein, is regulated by dietary restriction and subsequent re-feeding in mice. Proc Biol Sci 2013;280:20130101.
13. Mattison JA, Roth GS, Beasley TM, Tilmont EM, Handy AM, Herbert RL, Longo DL, Allison DB, Young JE, Bryant M, Barnard D, Ward WF, Qi W, Ingram DK, de Cabo R. Impact of caloric restriction on health and survival in rhesus monkeys from the NIA study. Nature 2012;489:318–321.
14. Walford RL, Mock D, Verdery R, MacCallum T. Calorie restriction in biosphere 2: alterations in physiologic, hematologic, hormonal, and biochemical parameters in humans restricted for a 2-year period. J Gerontol A Biol Sci Med Sci 2002;57:B211–B224.
15. Fontana L, Meyer TE, Klein S, Holloszy JO. Long-term calorie restriction is highly effective in reducing the risk for atherosclerosis in humans. Proc Natl Acad Sci USA 2004;101:6659–6663.
16. Bodkin NL, Alexander TM, Ortmeyer HK, Johnson E, Hansen BC. Mortality and morbidity in laboratory-maintained rhesus monkeys and effects of long-term dietary restriction. J Gerontol A Biol Sci Med Sci 2003;58:212–219.
17. Messaoudi I, Warner J, Fischer M, Park B, Hill B, Mattison J, Lane MA, Roth GS, Ingram DK, Picker LJ, Douek DC, Mori M, Nikolich-Zugich J. Delay of T cell senescence by caloric restriction in aged long-lived nonhuman primates. Proc Natl Acad Sci USA 2006;103:19448–19453.
18. Colman RJ, Anderson RM, Johnson SC, Kastman EK, Kosmatka KJ, Beasley TM, Allison DB, Cruzen C, Simmons HA, Kemnitz JW, Weindruch R. Caloric restriction delays disease onset and mortality in rhesus monkeys. Science 2009;325:201–204.
19. Colman RJ, Beasley TM, Allison DB, Weindruch R. Attenuation of sarcopenia by dietary restriction in rhesus monkeys. J Gerontol A Biol Sci Med Sci 2008;63:556–559.
20. Austad SN. Ageing: Mixed results for dieting monkeys. Nature 2012;489:210–211.
21. Stein PK, Soare A, Meyer TE, Cangemi R, Holloszy JO, Fontana L. Caloric restriction may reverse age-related autonomic decline in humans. Aging Cell 2012;11:644–650.
22. Verdery RB, Walford RL. Changes in plasma lipids and lipoproteins in humans during a 2-year period of dietary

restriction in Biosphere 2. Arch Intern Med 1998;158: 900–906.
23. Yang ZH, Miyahara H, Takeo J, Katayama M. Diet high in fat and sucrose induces rapid onset of obesity-related metabolic syndrome partly through rapid response of genes involved in lipogenesis, insulin signalling and inflammation in mice. Diabetol Metab Syndr 2012;4:32.
24. Lublinsky S, Luu YK, Rubin CT, Judex S. Automated separation of visceral and subcutaneous adiposity in in vivo microcomputed tomographies of mice. J Digit Imaging 2009;22:222–231.
25. Boesch-Saadatmandi C, Wagner AE, Wolffram S, Rimbach G. Effect of quercetin on inflammatory gene expression in mice liver in vivo—role of redox factor 1, miRNA-122 and miRNA-125b. Pharmacol Res 2012;65:523–530.
26. Hara A, Radin NS. Lipid extraction of tissues with a low-toxicity solvent. Anal Biochem 1978;90:420–426.
27. Gurtler A, Kunz N, Gomolka M, Hornhardt S, Friedl AA, McDonald K, Kohn JE, Posch A. Stain-free technology as a normalization tool in Western blot analysis. Anal Biochem 2013;433:105–111.
28. Wu B, Gu MJ, Heydari AR, Richardson A. The effect of age on the synthesis of two heat shock proteins in the hsp70 family. J Gerontol 1993;48:B50–B56.
29. Heydari AR, Conrad CC, Richardson A. Expression of heat shock genes in hepatocytes is affected by age and food restriction in rats. J Nutr 1995;125:410–418.
30. Gutman R, Yosha D, Choshniak I, Kronfeld-Schor N. Two strategies for coping with food shortage in desert golden spiny mice. Physiol Behav 2007;90:95–102.
31. Cui M, Yu H, Wang J, Gao J, Li J. Chronic caloric restriction and exercise improve metabolic conditions of dietary-induced obese mice in autophagy correlated manner without involving AMPK. J Diabetes Res 2013;2013: 852754.
32. Park S, Park NY, Valacchi G, Lim Y. Calorie restriction with a high-fat diet effectively attenuated inflammatory response and oxidative stress-related markers in obese tissues of the high diet fed rats. Mediators Inflamm 2012; 2012:984643.
33. Duivenvoorde LP, van Schothorst EM, Bunschoten A, Keijer J. Dietary restriction of mice on a high-fat diet induces substrate efficiency and improves metabolic health. J Mol Endocrinol 2011;47:81–97.
34. Petro AE, Cotter J, Cooper DA, Peters JC, Surwit SJ, Surwit RS. Fat, carbohydrate, and calories in the development of diabetes and obesity in the C57BL/6J mouse. Metabolism 2004;53:454–457.
35. Kalupahana NS, Voy BH, Saxton AM, Moustaid-Moussa N. Energy-restricted high-fat diets only partially improve markers of systemic and adipose tissue inflammation. Obesity (Silver Spring) 2011;19:245–254.
36. Blagosklonny MV. Calorie restriction: Decelerating mTOR-driven aging from cells to organisms (including humans). Cell Cycle 2010;9:683–688.
37. Zoncu R, Efeyan A, Sabatini DM. mTOR: From growth signal integration to cancer, diabetes and ageing. Nat Rev Mol Cell Biol 2011;12:21–35.
38. Cuervo AM, Dice JF. Age-related decline in chaperone-mediated autophagy. J Biol Chem 2000;275:31505–31513.
39. Cuervo AM. Autophagy and aging: Keeping that old broom working. Trends Genet 2008;24:604–612.
40. Heydari AR, Wu B, Takahashi R, Strong R, Richardson A. Expression of heat shock protein 70 is altered by age and diet at the level of transcription. Mol Cell Biol 1993;13: 2909–2918.
41. Zhang C, Cuervo AM. Restoration of chaperone-mediated autophagy in aging liver improves cellular maintenance and hepatic function. Nat Med 2008;14:959–965.
42. Spindler SR, Crew MD, Mote PL, Grizzle JM, Walford RL. Dietary energy restriction in mice reduces hepatic expression of glucose-regulated protein 78 (BiP) and 94 mRNA. J Nutr 1990;120:1412–1417.
43. Dhahbi JM, Mote PL, Tillman JB, Walford RL, Spindler SR. Dietary energy tissue-specifically regulates endoplasmic reticulum chaperone gene expression in the liver of mice. J Nutr 1997;127:1758–1764.
44. Dhahbi JM, Cao SX, Tillman JB, Mote PL, Madore M, Walford RL, Spindler SR. Chaperone-mediated regulation of hepatic protein secretion by caloric restriction. Biochem Biophys Res Commun 2001;284:335–339.
45. Ozcan U, Ozcan L, Yilmaz E, Duvel K, Sahin M, Manning BD, Hotamisligil GS. Loss of the tuberous sclerosis complex tumor suppressors triggers the unfolded protein response to regulate insulin signaling and apoptosis. Mol Cell 2008;29:541–551.
46. Pfaffenbach KT, Nivala AM, Reese L, Ellis F, Wang D, Wei Y, Pagliassotti MJ. Rapamycin inhibits postprandial-mediated X-box-binding protein-1 splicing in rat liver. J Nutr 2010;140:879–884.
47. Pfaffenbach KT, Pong M, Morgan TE, Wang H, Ott K, Zhou B, Longo VD, Lee AS. GRP78/BiP is a novel downstream target of IGF-1 receptor mediated signaling. J Cell Physiol 2012;227:3803–3811.
48. Um SH, Frigerio F, Watanabe M, Picard F, Joaquin M, Sticker M, Fumagalli S, Allegrini PR, Kozma SC, Auwerx J, Thomas G. Absence of S6K1 protects against age- and diet-induced obesity while enhancing insulin sensitivity. Nature 2004;431:200–205.
49. Khamzina L, Veilleux A, Bergeron S, Marette A. Increased activation of the mammalian target of rapamycin pathway in liver and skeletal muscle of obese rats: Possible involvement in obesity-linked insulin resistance. Endocrinology 2005;146:1473–1481.
50. Hagiwara A, Cornu M, Cybulski N, Polak P, Betz C, Trapani F, Terracciano L, Heim MH, Ruegg MA, Hall MN. Hepatic mTORC2 activates glycolysis and lipogenesis through Akt, glucokinase, and SREBP1c. Cell Metab 2012; 15:725–738.
51. Wang RH, Kim HS, Xiao C, Xu X, Gavrilova O, Deng CX. Hepatic Sirt1 deficiency in mice impairs mTorc2/Akt signaling and results in hyperglycemia, oxidative damage, and insulin resistance. J Clin Invest 2011;121:4477–4490.
52. Walsh ME, Shi Y, Van Remmen H. The effects of dietary restriction on oxidative stress in rodents. Free Radic Biol Med 2014;66:88–99.
53. Blagosklonny MV. Aging: ROS or TOR. Cell Cycle 2008; 7:3344–3354.
54. Mendelsohn AR, Larrick JW. Dissecting mammalian target of rapamycin to promote longevity. Rejuvenation Res 2012;15:334–337.
55. Wang C, Maddick M, Miwa S, Jurk D, Czapiewski R, Saretzki G, Langie SA, Godschalk RW, Cameron K, von Zglinicki T. Adult-onset, short-term dietary restriction reduces cell senescence in mice. Aging (Albany NY) 2010;2:555–566.
56. Thondamal M, Witting M, Schmitt-Kopplin P, Aguilaniu H. Steroid hormone signalling links reproduction to

lifespan in dietary-restricted *Caenorhabditis elegans*. Nat Commun 2014;5:4879.
57. Mucignat-Caretta C, Caretta A, Cavaggioni A. Acceleration of puberty onset in female mice by male urinary proteins. J Physiol 1995;486(Pt 2):517–522.
58. Hui X, Zhu W, Wang Y, Lam KS, Zhang J, Wu D, Kraegen EW, Li Y, Xu A. Major urinary protein-1 increases energy expenditure and improves glucose intolerance through enhancing mitochondrial function in skeletal muscle of diabetic mice. J Biol Chem 2009;284:14050–14057.

Address correspondence to:
Patricia Huebbe
Institute of Human Nutrition and Food Science
H. Rodewald Strasse 6
24118 Kiel
Germany

E-mail: huebbe@foodsci.uni-kiel.de

Received: October 10, 2014
Accepted: November 18, 2014